Endocrine Journal 2014, **61** (6), 615-621

ORIGINAL

Phantom experiment and clinical utility of quantitative shear wave elastography for differentiating thyroid nodules

Takahiro Fukuhara[1)], Eriko Matsuda[1)], Kazunori Fujiwara[1)], Chika Tanimura[2)], Shoichiro Izawa[3)], Hideyuki Kataoka[2)] and Hiroya Kitano[1)]

[1)] *Department of Otolaryngology-Head and Neck Surgery, Tottori University Faculty of Medicine, Yonago 683-8504, Japan*
[2)] *Department of Adult and Elderly Nursing, Tottori University Faculty of Medicine, Yonago 683-8504, Japan*
[3)] *Endocrinology and Metabolism, Department of Molecular Medicine and Therapeutics, Tottori University Faculty of Medicine, Yonago 683-8504, Japan*

Abstract. Shear wave elastography (SWE) using acoustic radiation force impulse (ARFI) is a novel ultrasonography technique. The aim of this study was to investigate the clinical usefulness of quantitative SWE for differentiating thyroid nodules. For phantom study, we measured the shear wave velocities (SWVs) of the four spheres of 2- and 1-cm diameters with varying hardness. For clinical study, the SWVs of normal thyroid glands and thyroid nodules, that were classified as benign or malignant according to either cytological or pathological findings, were measured. The SWVs of each thyroid patient were compared with that of a normal thyroid and each other. In phantom study, the SWVs for the 2-cm spheres correlated with the hardness of the targets, whereas the values for the 1-cm spheres did not. In clinical study, 112 nodules identified in 167 patients and 94 normal thyroid glands were analyzed according to the criteria for the study. The nodules included 84 benign nodules, and 28 papillary carcinoma. The mean SWVs of each group were 1.64 ± 0.47 m/s for normal thyroid, 1.88 ± 0.62 m/s for benign nodules and 2.67 ± 0.76 m/s for papillary carcinoma. The SWVs of papillary carcinoma were significantly higher than those of benign nodules ($P < 0.001$). The area under the ROC curve was 0.809 with a cut-off value of 2.01 m/s. The sensitivity and specificity were 85.7% and 62.0% respectively. Results showed that SWE provides new information on tumor characteristics, such as hardness and larger nodules tended to provide stable measurements.

Keywords: Shear wave, Quantitative elastography, Acoustic radiation force impulse, Thyroid nodule, Ultrasound

RECENTLY ULTRASONOGRAPHY EQUIPMENT has remarkably improved. High-resolution ultrasonography excels in the detection of thyroid lesions, and it is an essential tool for diagnosing thyroid diseases. The present of specific features on B-mode sonography, evaluation of blood flow with Doppler sonography, and the strain ratio measured by strain elastography (SE) provide predictions of tissue characteristics to a certain degree. However, ultrasonography remains suboptimal for diagnosing thyroid diseases [1, 2].

The novel technology of shear wave elastography (SWE), also known as virtual touch quantification (VTQ), can measure the shear wave velocity (SWV) caused by acoustic radiation force impulse (ARFI). Using Young's modulus, the velocity directly reflects the tissue hardness. Thus, SWE has the potential to quantitatively evaluate the tissue hardness. For evaluation of the tissue hardness, SE imaging is a well-known technique. SE measures the strain ratio of tissues in the region of interest (ROI). Therefore, the evaluation is a relative estimate, and it is limited to the ROI on one side of the neck. In addition, sonographers have a significant effect on the diagnoses [3, 4]. Compared with SE, SWE is a quantitative and not an operator-dependent method that avoids the limitation of SE for the head and neck region, including the thyroid [5-8]. Therefore, SWE is expected to provide more information. However, only limited clinical patient data on patients for the head and neck region are available, because SWE is a new system. The aim of this study

Submitted Feb 10, 2014; Accepted Mar. 11, 2014 as EJ14-0061
Released online in J-STAGE as advance publication Apr. 8, 2014
Correspondence to:Takahiro Fukuhara, M.D., Ph.D., Department of Otolaryngology-Head and Neck Surgery, Tottori University Faculty of Medicine, 36-1, Nishicho, Yonago, 683-8504, Japan.
E-mail: tfukuhara3387@med.tottori-u.ac.jp

was to perform the phantom experiment and investigate the clinical usefulness of SWE for differentiating thyroid nodules.

Patients and Methods

Phantom study

For the phantom study, we used a commercially available Elasticity QA Phantom Model 049 (CIRS, Nolfolk, VA, USA). Four spheres of both 2- and 1-cm diameters with varying hardness were embedded. The depth of the 2-cm spheres from the surface to the sphere center was 3.3 cm, while the depth of the 1-cm spheres was 1.4 cm. The hardness level of the spheres and background were as follows: lesion type 1, 8 kpa; lesion type 2, 14 kpa; lesion type 3, 45 kpa; lesion type 4, 80 kpa; and background, 25 kpa. We measured the SWV (m/s) for the four spheres of each size and the background at each depth for the phantom. With the ROI set at the center of a target, the measurement was repeated for five times.

Patients

Informed consent was obtained from the patients, and the study was performed in accordance with the ethical guidelines of the Helsinki Declaration. The institutional review board of Tottori University approved the study protocol. The study was conducted between November 2011 and April 2013. We included patients with thyroid nodules who had undergone an ultrasound examination for screening or further evaluation of the thyroid gland at our otolaryngology-head and neck surgery department. Patients were then screened to determine whether they satisfied the inclusion criteria for this study listed below. The nodules were classified as either benign or malignant and then compared with the normal thyroid glands and with each other. The each inclusion criteria for the study were as follows.

Criteria

The normal thyroid group had normal imaging on ultrasonography, with normal serum thyroid hormone levels (TSH, FT3, and FT4). The thyroid nodules were ≥10-mm diameter that were performed fine needle aspiration biopsy (FNAB) of thyroid nodules and examined their cytology, and/or histopathology by surgery. Benign nodules included goiter nodules and adenomas. Diffuse goiters were excluded. Exclusion criteria were cystic lesions, multiple small nodules.

FNAB/ surgery

FNAB was performed on ≥10-mm diameter nodules. The nodules were then classified as either benign or malignant according to either cytological or pathological findings. It is possible that a small number of follicular carcinoma have benign cytology, and in this study they would have been classified as benign nodules, except when pathologically diagnosed as follicular carcinoma, after surgery. Patients with nodules of indeterminate cytology by FNAB without confirmation by surgery were excluded.

Measurement procedures

The thyroid glands of all the patients were examined using the ACUSON S2000 ultrasound system (Siemens Medical Systems, Mountein View, CA, USA) with a B-mode-ARFI combination linear transducer (9L4; Siemens Medical Solutions). The location, size, echo pattern, and vascularity were observed for each lesion. To perform SWE on B-mode US images, a target region with a fixed dimension of 5 x 5 mm was identified as the region of interest (ROI). An acoustic push pulse was transmitted and a shear wave generated in the target region. The shear waves were detected by sonographic detection pulses, and the numerical values of the SWE were displayed. We applied the SWE to the right and/or left lobe of the thyroid gland and to the solid parts of the thyroid tumors. The probe was axially pushed lightly into the neck. The 5-mm square ROI was placed within the entire thyroid lesion (Fig. 1): five measurements were then performed at the same point. The mean of the five measurements for each thyroid patient was compared with that of a normal indi-

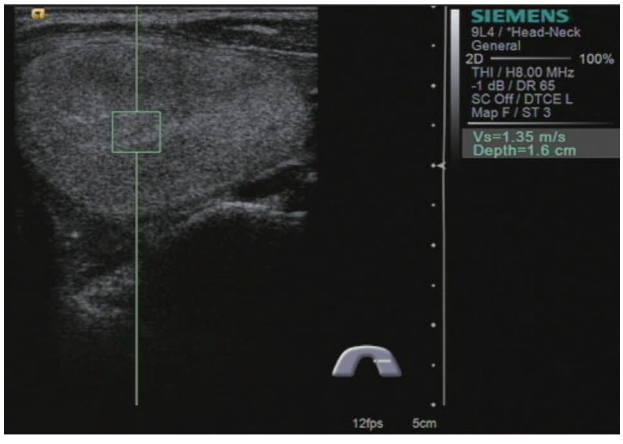

Fig. 1 The 5-mm square ROI within the entire thyroid lesion

vidually.

In SWE, the SWV was expressed in m/s. Only numerical results were taken into consideration. When the measurements showed X.XX m/s and five times of numeric results could not be recorded, we regarded the objects as unmeasurable lesions.

Statistical analysis

Statistical analyses were performed using SSPS software (IBM SPSS Statistics 21; IBM, Japan). First, we calculated the ratios between measurable and unmeasurable lesions in each group with normal tissue, benign nodules, or malignant nodules. The data of measurable lesions were expressed as the mean ± standard deviation (SD).

The groups with normal tissue, benign nodules, or malignant nodules were compared with each other using either Student's *t*-test or the Mann−Whitney U test. The diagnostic performance was assessed using receiver operating characteristic curves (ROC curves), and the optimal cut-off values were calculated using Youden's index. The correlations between tumor diameter and SD of the five measurements were assessed by Pearson's correlation coefficient. For unmeasurable malignant nodules, the ultrasonographic features of thyroid cancer were assessed using the χ^2 test.

Results

Phantom study

The results are shown in Table 1. The mean SWVs for sphere types 1−4 of smaller size (1-cm diameters) and background at 1.4-cm depth, was 1.74 m/s (range, 1.72−1.75 m/s; SD, 0.01), 2.04 m/s (range, 2.01−2.06 m/s; SD, 0.02), 2.84 m/s (range, 2.47−3.02 m/s; SD, 0.23), 2.00 m/s (range, 1.95−2.11; SD, 0.06), and 2.62 m/s (range, 2.61−2.65 m/s; SD, 0.02) respectively. The mean SWVs for sphere types 1−4 of 2.0-cm diameter and background at 3.3-cm depth, were 1.36 m/s (range, 1.32−1.40 m/s; SD, 0.03), 1.90 m/s (range, 1.88−1.93 m/s; SD, 0.02), 3.46 m/s (range, 3.43−3.47 m/s; SD, 0.03), 5.22 m/s (range, 5.18−5.24; SD, 0.02), and 2.54 m/s (range, 2.50−2.57 m/s; SD, 0.03), respectively. For 2-cm spheres, the measurements closely reflect the hardness of the targets. The SWVs for the bigger spheres correlated with the hardness of the targets, whereas the values for the smaller, hard spheres (types 3 and 4) of 1-cm diameter did not relate to their hardness. The depth of the measurements may not have materially affected the results.

Clinical evaluation

A total of 336 patients were underwent ultrasonographic examinations according to the study protocol, with 112 nodules and 94 normal glands identified in 167 patients (males, 56; females, 111; mean age, 59 years; range, 12−91 years) analyzed according to the criteria for the study. The groups included 94 normal thyroids glands, 84 cases with benign nodules, and 28 cases with malignant nodules. Characteristics of all cases are shown in Table 2. All nodules were diagnosed by FNAB cytology and/or surgery. All malignant nodules were papillary carcinomas. The measurable ratios of each group were 100% for normal thyroids glands, 94% for benign nodules, and 50% for papillary carcinoma (Table 3). The mean SWVs of each group were as follows: 1.64 ± 0.47 m/s for normal thyroid glands, 1.88 ± 0.62 m/s for benign nodules, and 2.67 ± 0.76 m/s for papillary carcinoma (Fig. 2). The SWVs of papil-

Table 1 Results of the Phantom Study. The hardness of each sphere and the mean shear wave velocities (SWVs) are shown. For 2-cm spheres, the measurements closely reflect the hardness of the targets

Sphere type	hardness (kpa)	SWVs of 1 cm sphere (m/s)	SWVs of 2 cm sphere (m/s)
type 1	8	1.74 ± 0.01	1.36 ± 0.03
type 2	14	2.04 ± 0.02	1.90 ± 0.02
background	25	2.62 ± 0.02	2.54 ± 0.03
type 3	45	2.84 ± 0.23	3.46 ± 0.03
type 4	80	2.00 ± 0.06	5.22 ± 0.02

Table 2 The number and characteristics of the patients in the study

	Normal	Benign	Malignant
Patient number	66	76	25
Case number	94	84	28
Sex (female/male)	32/34	60/16	19/6
Age (yrs)	59 ± 18	59 ± 17	59 ± 17
Age range (yrs)	12-91	16-93	24-79

Table 3 The number and ratio of measurable and unmeasurable cases in each group

	N*	Measurable	Unmeasurable	Measurable ratio (%)
Normal	94	94	0	100
Benign	84	79	5	94
Malignant	28	14	14	50

* N: number of cases.

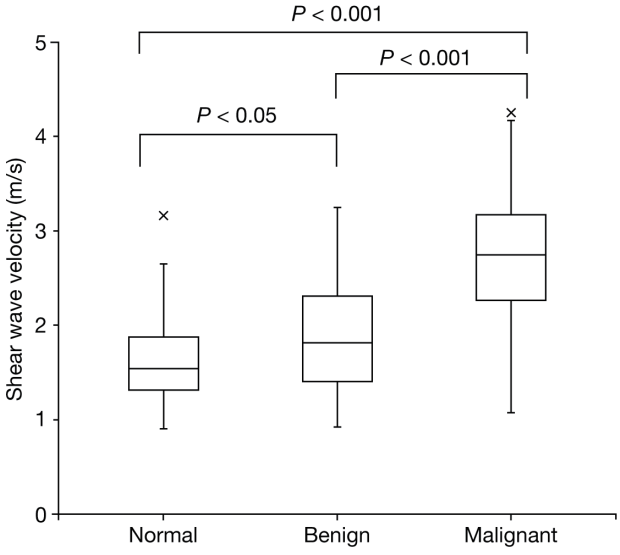

Fig. 2 Box-and-whisker plots of the shear wave velocities (SWVs) measured in normal thyroid glands, benign nodules, and malignant nodules. × means outlier.

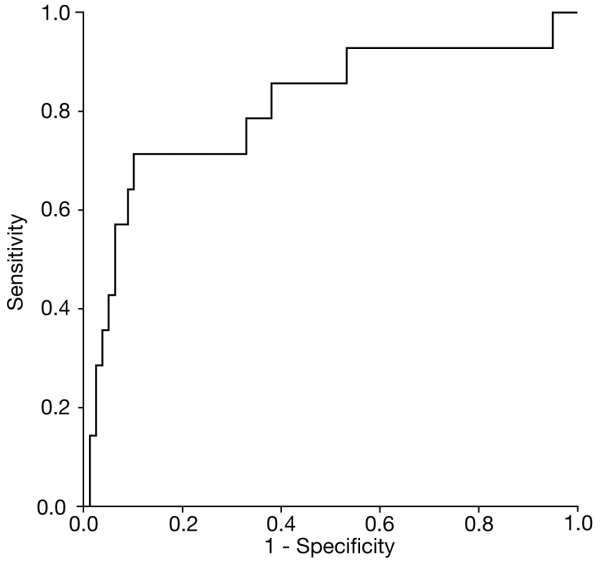

Fig. 3 Receiver Operating Characteristic (ROC) curve for differentiating between benign and malignant nodules using shear wave velocities (SWVs) measurements.

Table 4 The results with the cut-off value of 2.01 m/s

	Papillary carcinoma	Benign nodules
SWV ≥ 2.01 m/s	24	32
SWV < 2.01 m/s	4	52

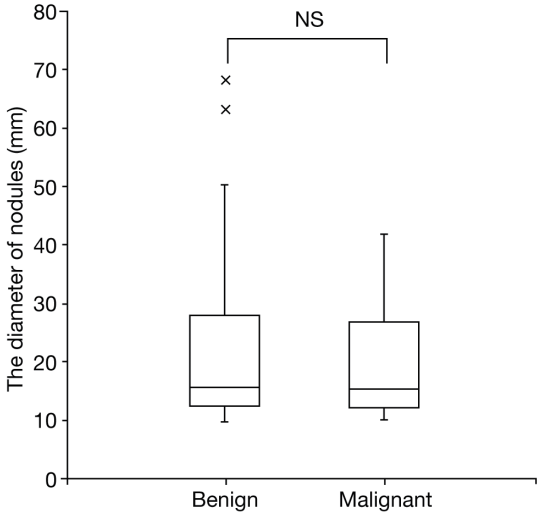

Fig. 4 Box-and-whisker plots of the diameters of benign and malignant nodules. × means outlier.

lary carcinoma were significantly higher than those of normal thyroids ($P < 0.001$). Analysis using the *t*-test showed that there was no significant difference in the SWVs between normal thyroid glands and benign nodules. Because the Levene's test showed that data of the benign nodules had unequal variance, we used the Mann−Whitney U test to analyze data of the benign nodules. This showed there was a significant difference between normal thyroid glands and benign nodules ($P < 0.05$).

The SWVs of papillary carcinoma were significantly higher than those of benign nodules ($P < 0.001$). As shown in Fig. 3, the area under the ROC curve was 0.809, and the cut-off value using Youden's index was 2.01 m/s. When the cut-off value was 2.01 m/s, the sensitivity, specificity, positive predictive value, negative predictive value, and diagnostic accuracy were 85.7%, 62.0%, 67.9%, 92.9% and 67.9%, respectively (Table 4). The diameter of individual benign and malignant nodules is shown in Fig. 4. The mean diameters of benign and malignant nodules were 21.2 mm ± 12.5 and 19.4 ± 9.9 mm, respectively. A weak negative correlation was observed between the tumor diameters of the benign nodules and SD of the five measurements, with a Pearson's correlation coefficient of –0.38 (Fig. 5a). There was no correlation between the tumor diameters of malignant nodules and SD of the five measurements, with a Pearson's correlation coefficient of –0.11 (Fig. 5b). Coarse calcification was one of the causes for unmeasurable papillary carcinoma observed during ultrasonography ($\chi^2 = 4.094$, $P < 0.05$). In contrast, a

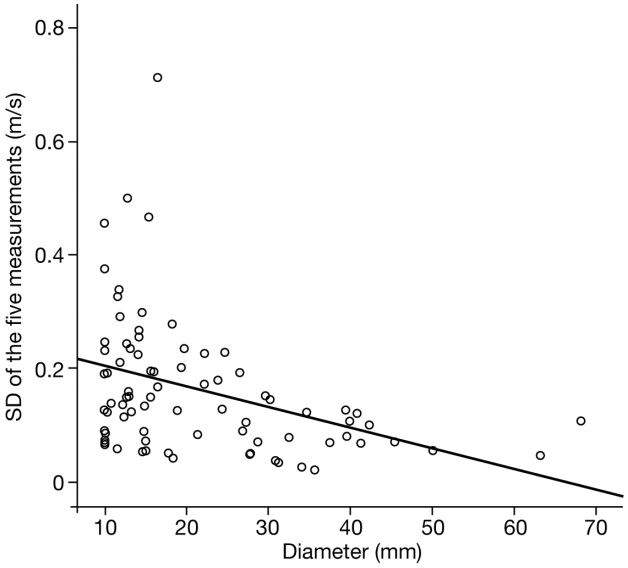

Fig. 5a Chart showing the correlation chart of correlation between the diameters of benign nodules and standard deviations of the five measurements (Pearson's correlation coefficient, −0.38).

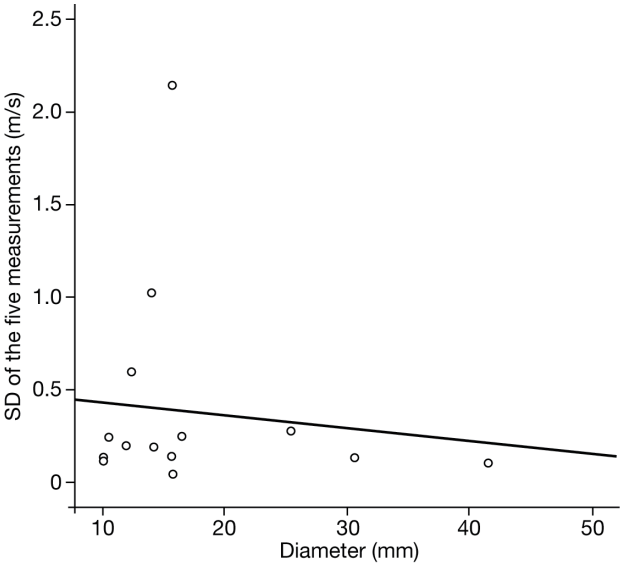

Fig. 5b Chart showing the correlation chart of correlation between the diameters of malignant nodules and standard deviations of the five measurements (Pearson's correlation coefficient, −0.11).

Table 5 The χ^2 tests for correlation between unmeasurable malignant nodules and ultrasound features of thyroid cancer: heterogeneous of internal echo, coarse calcification, and marked intranodular blood flow

	Heterogeneous		Coarse calcification		Type 3 blood flow	
	Yes	No	Yes	No	Yes	No
N*	21	7	9	19	12	15
Measurable	9	5	2	12	4	9
Unmeasurable	12	2	7	7	8	6
χ^2 value	1.714		4.094		1.899	
P value	0.190		< 0.05		0.168	

*N: number of cases

heterogeneous internal echo and type 3 blood flow or marked intranodular blood flow [9], were not causes of the unmeasurable state (χ^2 = 1.714, P = 0.190; χ^2 = 1.899, P = 0.168, respectively) (Table 5).

Discussion

The advantages of SWE are that is a simple, quantitative method with no self-judgment required by sonographers. We observed a significant difference between benign nodules and papillary carcinoma, with the results indicating that SWE could provide new information on tumor characteristics, such as hardness.

However, numerical results could not be measured in 50% papillary carcinoma. When SWV can not be calculated in SWE, "X.XX" is displayed on the monitor [10, 11]. There are various interpretations of "X.XX" [5, 10, 12-15], with a major view being that "X.XX" represents the SWVs that exceed the range of 1−10 m/s for SWE [5, 10, 12]. In their study, Bojunga *et al*. substituted numerical values of 8.4 m/s, when "X.XX" was displayed on the monitor [5]. However, it remains unclear what value should be used when "X.XX" is expressed.

We considered the relationship between nodule size and the availability of SWV measurements. In the phantom study, the small, hard type 3 and 4 spheres did not provide consistent measurements, whereas, the measurements of all the 2-cm spheres reflected their hardness. Clinical evaluation of the benign nodules showed

that bigger nodule diameters had smaller SDs for the five measurements. Zhang *et al*. also demonstrated that the diagnostic performance of SWV for differentiating benign from malignant thyroid nodules improved when the nodules had a diameter of >20 mm [8]. In contrast, when the nodules had small diameters, SWV measurements were not stable. The ultrasonic waves of the push pulse that were reflected and refracted at the curved boundaries of the nodules, resulting in irregular production of shear waves, were thought be responsible for this depreciation. On the other hand, in SE, the strain ratio of large tumors compared with that of the surrounding tissue cannot be measured because the tumor size is greater than the ROI of elastography [16, 17]. SWE may avoid this limitation of elastography imaging.

However, the nodule size may be just one of the causes for measurement error because 50% of papillary carcinoma were unmeasurable compared with approximately all benign nodules that were measurable, despite no differences in the nodule size between the two types of lesions. The current study found that coarse calcification is one malignant feature that influences measurement error on B-mode sonography. Therefore, we considered that SWVs were affected by the pathological structures of the targets. In the ACUSON S2000 ultrasound system, SW is detected at numbers of points within ROI and then the velocity of SW is calculated. When the SWV is not constant within ROI, the velocity is not able to be calculated. We thought this was one of reasons why the measured value of tissue with mixed structure became error. Conversely, because the majority of malignant nodules show "X.XX" on the monitor, it is likely that the unmeasurable state may be a characteristic feature of malignant nodules. The limitations of this study were that all malignant nodules were papillary carcinomas; therefore, differentiation between follicular adenoma and follicular carcinoma remained unclear, and half of papillary carcinoma were unmeasurable.

The SWVs of benign nodules did not significantly differ from those measured in normal thyroid glands and the causes for measurement error of papillary carcinoma has been unclear. Therefore, further studies are required to determine the correlation between SWV and pathology of the targets as well as measurement artifacts.

Acknowlegments

We would like to thank Masahiro Saito (Mochida Siemens Medical Systems Co., Ltd., Tokyo, Japan) for his technical advice.

Disclosure Statement

The authors declare that no competing financial interests exist.

References

1. Bojunga J, Herrmann E, Meyer G, Weber S, Zeuzem S, et al. (2010) Real-time elastography for the differentiation of benign and malignant thyroid nodules: a meta-analysis. *Thyroid* 20: 1145−1150.
2. Lippolis PV, Tognini S, Materazzi G, Polini A, Mancini R, et al. (2011) Is elastography actually useful in the presurgical selection of thyroid nodules with indeterminate cytology? *J Clin Endocrinol Metab* 96: 1826−1830.
3. Burnside ES, Hall TJ, Sommer AM, Hesley GK, Sisney GA, et al. (2007) Differentiating benign from malignant solid breast masses with US strain imaging. *Radiology* 245: 401−410.
4. Regner DM, Hesley GK, Hangiandreou NJ, Morton MJ, Nordland MR, et al. (2006) Breast lesions: evaluation with US strain imaging- clinical experience of multiple observers. *Radiology* 238: 425−437.
5. Bojunga J, Dauth N, Berner C, Meyer G, Holzer K, et al. (2012) Acoustic radiation force impulse imaging for differentiation of thyroid nodules. *PLoS One* 7: e42735.
6. Lyshchik A, Higashi T, Asato R, Tanaka S, Ito J, et al. (2005) Thyroid gland tumor diagnosis at US elastography. *Radiology* 237: 202−211.
7. Rago T, Santini F, Scutari M, Pinchera A, Vitti P (2007) Elastography: new development in ultrasound for predicting malignancy in thyroid nodules. *J Clin Endocrinol Metab* 92: 2917−2922.
8. Zhang YF, Xu HX, He Y, Liu C, Guo LH, et al. (2012) Virtual touch tissue quantification of acoustic radiation force impulse: a new ultrasound elastic imaging in the diagnosis of thyroid nodules. *PLoS One* 7: e49094.
9. Rago T, Vitti P, Chiovato L, Mazzeo S, De Liperi A, et al. (1998) Role of conventional ultrasonography and color flow-doppler sonography in predicting malignancy in "cold" thyroid nodules. *Eur J Endocrinol* 138: 41−46.
10. Tozaki M, Saito M, Joo C, Yamaguchi M, Isobe S, et al. (2011) Ultrasonographic tissue quantification of

the breast using acoustic radiation force impulse technology: phantom study and clinical application. *Jpn J Radiol* 29: 598−603.
11. Benson J, Fan L. (2011) Tissue strain analysis: a complete ultrasound solution for elastography. *Available at* www.healthcare.siemens.com/. Accessed November 20.
12. Gu J, Du L, Bai M, Chen H, Jia X, et al. (2012) Preliminary study on the diagnostic value of acoustic radiation force impulse technology for differentiating between benign and malignant thyroid nodules. *J Ultrasound Med* 31: 763−771.
13. Bai M, Du L, Gu J, Li F, Jia X (2012) Virtual touch tissue quantification using acoustic radiation force impulse technology: Initial clinical experience with solid breast masses. *J Ultrasound Med* 31: 289−294.
14. Hou XJ, Sun AX, Zhou XL, Ji Q, Wang HB, et al. (2013) The application of virtual touch tissue quantification (VTQ) in diagnosis of thyroid lesions: a preliminary study. *Eur J Radiol* 82: 797−801.
15. Tozaki M, Isobe S, Fukuma E (2011) Preliminary study of ultrasonographic tissue quantification of the breast using the acoustic radiation force impulse (ARFI) technology. *Eur J Radiol* 80: 182−187.
16. Itoh A, Ueno E, Tohno E, Kamma H, Takahashi H, et al. (2006) Breast disease: clinical application of US elastography for diagnosis. *Radiology* 239: 341−350.
17. Raza S, Odulate A, Ong EM, Chikarmane S, Harston CW (2010) Using real-time tissue elastography for breast lesion evaluation. *J Ultrasound Med* 29: 551−563.